# Study of Physically Transient Insulating Materials as a Potential Platform for Transient Electronics and Bioelectronics

*Handan Acar, Simge Çınar, Mahendra Thunga, Michael R. Kessler, Nastaran Hashemi, and Reza Montazami**

**Controlled degradation and transiency of materials is of significant importance in the design and fabrication of degradable and transient biomedical and electronic devices and platforms. Here, the synthesis of programmable biodegradable and transient insulating polymer films is reported, which have sufficient physical and chemical properties to be used as substrates for the construction of transient electronics. The composite structure can be used as a means to control the dissolution and transiency rate of the polymer composite film. Experimental and computational studies demonstrate that the addition of gelatin or sucrose to a PVA polymer matrix can be used as a means to program and either slow or enhance the transiency of the composite. The dissolution of the polymer composites are fitted with inverse exponential functions of different time constants; the lower time constants are an indication of faster transiency of the polymer composite. The addition of gelatin results in larger time constants, whereas the addition of sucrose generally results in smaller time constants.**

## 1. Introduction

Degradable materials play a critically important role in modern implantable organic bioelectronics;[1] and, contribute significantly to advances in the new field of transient electronics.[2] Research on organic bioelectronics based on silicon nano-membranes,[3] and peptide templates,[4] with emphasis on device-tissue interface, has gained tremendous momentum in the last decade. Unlike some biomedical devices such as pacemakers and artificial joints that are designed to last for an extended duration of time, degradable bioelectronic and biomedical devices are designed to undergo degradation after a relatively short period of time. Degradation duration varies, depending on the application. For instance, resorbable sutures should retain their mechanical properties for at least several days whereas targeted-drug-delivery vehicles are usually designed to instantaneously breakdown when exposed to the stimuli. It is of significant importance to design and fabricate degradable materials with tunable degradation, which can undergo quick and complete degradation when triggered. The term "transient materials" has been used to describe this class of programmable degradable materials.

Developing transient materials and devices holds tremendous value in biomedical, military and intelligence applications. For example, in one study transient materials have been used to provide thermal therapy to control surgical site infection as nano-antibiotic.[5] Many brain damages and abnormal brain activities can be detected and monitored by study of electric signal at the surface of the brain.[6,7] In one example, Kim et al. have demonstrated monitor of brain activities in a cat using dissolvable flexible electronics consisting of arrays of micro-fabricated electrodes.[7] In this open-skull procedure, electric signals were detected at the surface of brain and transmitted to a monitoring device where data was recorded and analyzed. This procedure could be performed as a closed-skull if the needs for monitor and removal of electrodes were eliminated by use of transient materials. Transient electronics can be used in this, or similar, cases where additional surgeries are required to remove biomedical devices from the body.[8] Flexible electronics are desirable for this type of studies, because they better conform to the 3-dimensionally curved structure of the organ. One important factor in design of bioelectronics is their interface

Dr. H. Acar, Dr. N. Hashemi, Dr. R. Montazami
Department of Mechanical Engineering
Iowa State, University
Ames, IA 50011, USA
E-mail: reza@iastate.edu
Dr. S. Çınar
Department of Materials Science and Engineering
Iowa State, University
Ames, IA 50011, USA
Dr. M. Thunga
Department of Chemistry
Iowa State, University
Ames, IA, 50011, USA
Ames Laboratory
US Department of Energy
Ames, IA, USA
Dr. M. R. Kessler
School of Mechanical and Materials Engineering
Washington State University
Pullman, WA 99164, USA

**DOI: 10.1002/adfm.201304186**

with the non-planar and non-static living tissue. Recently, progress has been made in this field concerning biodegradability, biocompatibility and bioresorbability of bio-organic electronic devices.[9,10] Also, considerable progress has been made in the direction of bioelectronics/living tissue interfaces with significant emphasis on mechanical properties of bioelectronics.[11,12] Typically, electronic components are fabricated on flexible platforms using photolithography[12] and surface modification[13] techniques.

Investigation of electronic devices based on transient materials (transient electronics) is a new and rarely addressed technology with paramount potentials in both medical and military applications. Each particular application, of course, requires some specific mechanical, chemical, physical and electrical properties. For instance, biomimicry and flexibility are essential properties for transient electronics designed to act as implantable biomedical devices and bioelectronics; whereas this characteristic may not be necessarily needed in military applications. To our best recollection, the first step towards biodegradable electronics have been reported by Bettinger et al. with a field-effect transistor based on poly(vinyl alcohol) (PVA) as gate dielectric, and 5,5′-bis-(7-dodecyl-9H-fluoren-2-(yl)-2,2′-bithiophene (DDFTTF) as organic semiconductor.[14] Although; poly(L-lactide-co-glycolide) (PLGA), a FDA approved polymer, was used as the biodegradable substrate, the degradation of the device took about 70 days at low-pH environment. In a recent study, biodegradable transistors were fabricated on peptide-based substrates, the system exhibited instant degradation when exposed to phosphate buffered saline (PBS), yet degradation rate was found to be not programmable.[15] Irimia et al. have investigated series of organic and biodegradable compounds that can serve as a platform for electronic components;[16] also have reported the use of caramelized sugar as a degradable materials with potential application in bio-organic degradable electronics.[9] As reported by the authors, the major problems with this approach were poor mechanical properties of caramelized sugar and the challenges in fabrication of electronic components on such material.

Currently, magnesium and magnesium-based materials are the most commonly used conductive transient materials. Magnesium and magnesium oxide are used in fabrication of conductive paths on electronic circuits as well as basic electronic components such as resistors and inductors through vapor deposition and direct assembly techniques. Magnesium is desirable because of its biocompatibility and most importantly, water solubility.[2,17] Progress on development of semi-conductors has been mainly focused on polymer-based and silicon nano-membrane-based electronics.[3] Also, peptide-based templates were used for development of semi-conductor nano-materials.[4] More recently, progress has been made in the direction of biological protonics and natural semiconductors. In a series of studies, Rolandi and colleagues have demonstrated biopolymer protonic field effect transistors functioning based on proton conduction.[18] In another series of studies, Sariciftci and colleagues have demonstrated semiconducting attributes of Indigo and Tyrian purple natural dyes;[19] also Mostert et al. have demonstrated ionic conductivity and semiconducting attributes of melanin and their dependence on the degrees of hydration of melanin.[20]

Efforts on investigating insulating materials as substrates for transient electronics, and more generally transient platforms, have been limited to couple of studies; in most cases the main focus had been on conductive-insulating systems. In one effort, Legnani et al. studied the bacterial cellulose membranes (BCM) to obtain flexible and biodegradable membranes for electronic devices.[21] Indium tin oxide (ITO) was deposited on BCM membranes to achieve efficient electrical conductivity. The platform was then used as the base for construction of an organic light emitting diode; the degradation of ITO coated BCM membrane took 70 days in acidic environment. In another study by Kim et al., silk fibroins was used in fabrication of ultra-thin membranes for bio-integrated electronics.[7] Silk-based membranes were also investigated by Hwang et al. as the insulating substrate for fabrication of Si-based and Mg-based transient electronics.[2] Degradation of silk membranes in PBS took about 10 min; however, Si-based electronics (<100 nm thick) only degraded in ample amount of PBS solution after several days. The degradation rate of the silk-based materials have been tuned by controlling the gelation time[22] and crystallization through physical temperature-controlled water vapor annealing.[23] Silk-based composites exhibit sufficient mechanical stability to allow fabrication of circuits, and high optical transparency that can be useful in some optical lithography techniques.

In our previous studies we have shown that electrical and mechanical properties of insulating, electrically conductive and ion permeable polymers can be manipulated via controlling the structure of polymer composites by integration of nano materials and/or filler polymers.[24]

In this study, we reported the investigation on insulating polymer composites and means for controlling the transiency rate in very short timespans. In this study, we investigated polymer composites consisting of PVA as polymer matrix; and, used sucrose and gelatin as fillers to program transiency rate of the blends. PVA was selected as the matrix polymer because of its biocompatibility, non-toxicity and desirable physical and chemical properties. Gelatin, a well-studied biocompatible substance that is obtained by a controlled hydrolysis of fibrous insoluble collagen,[25–27] was used as a mean to control transiency of the polymer composites. Depending on the PVA-gelatin ratio, the resultant composites may or may not be soluble. The strength of the PVA-gelatin film is due to the presence of triple helixes in gelatin structure.[26] The greater the triple helix content is, the higher the strength of the film and lower swelling and solubility are. Sucrose was used to enhance dissolution and also as a plasticizer to improve mechanical properties of the composite for biomedical applications.[28,29]

## 2. Results and Discussion

### 2.1. Thermal and Mechanical Analysis

The effects of chemical composition on thermal and mechanical properties of samples, specifically mechanical stiffness and phase behavior of polymer composites, were investigated. Elastic ($E$) and storage ($E'$) moduli of the polymer films were measured and the loss ($E''$) modulus was deduced from the

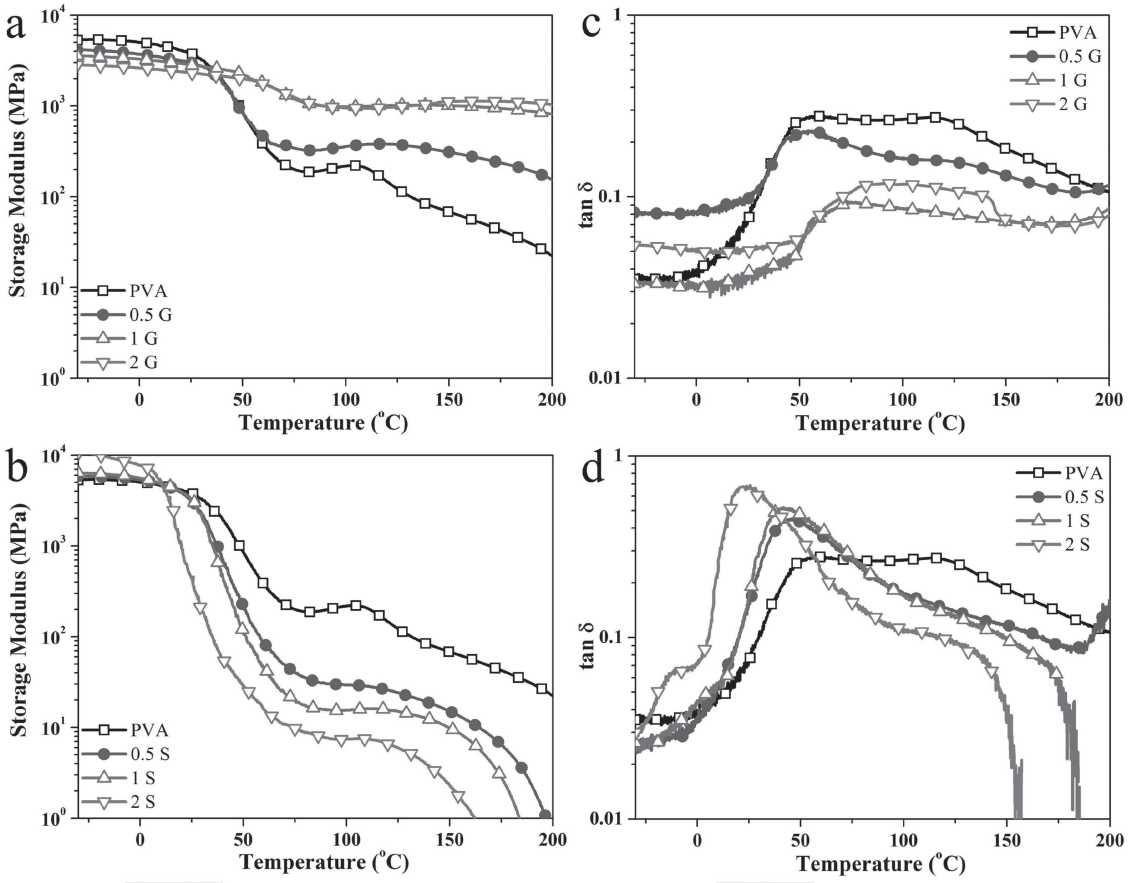


**Figure 1.** a,b) Temperature-dependent storage moduli, and c,d) tan $\delta$ curves of PVA/Gelatin and PVA/Sucrose samples, respectively.

data. The *tan* $\delta$ values, the ratios of loss to storage moduli ($E''$/E′) were plotted, which shows the transition dynamics of the polymer chain with the glass transition temperature ($T_g$) value.

The elastic modulus and *tan* $\delta$ curves of pure PVA and PVA/gelatin composites are shown in **Figure 1**a and b. Pure PVA is known to have several $T_g$ values depending on the degree of crosslinking and humidity.[30] The significant decrease at storage modulus in Figure 1a, and the pronounced peak in *tan* $\delta$ curve in Figure 1b at 50 °C correspond to the primary $T_g$ relaxation of pure PVA. Cascone et al.[31] have studied the phase behavior in PVA/gelatin composites using DMA and reported that, gelatin is stiffer than PVA over a broad temperature range and the $T_g$ of gelatin was observed above 200 °C. Similarly, increasing the concentration of gelatin in the composites resulted in shifting the $T_g$ of PVA phase to higher temperatures along with a simultaneous decrease in the intensity of the peaks. Thus, the peak at that region in the *tan* $\delta$ curves of PVA/gelatin composites were attributed to the $T_g$ of PVA phase (Figure 1b), which confirms miscibility between PVA and gelatin phases in the composites. From DMA curves, characterizing the $T_g$ of gelatin is difficult as the melt transition in PVA appears to overlap with the glass transition of gelatin phase at high temperature (above 180 °C).

A nominal decrease in the glassy modulus, storage modulus at $T < T_g$, of the gelatin composites was observed with the increase in the gelatin concentration above 2.5 wt% gelatin (0.5 G). At this concentration, gelatin likely commences to form continuous phase. The decrease in the glassy modulus of the composites was attributed to the influence of gelatin continuous phase on the crystallinity of PVA phase. On the other hand, above $T_g$ of PVA, the modulus of the material increased with increasing gelatin concentration in the blends. This observation is in agreement with the previous results.[27,31] As the gelatin segments are glassy at the $T_g$ of PVA, an obvious hindrance to the mobility of composite material was expected. Therefore, the shift in $T_g$ to higher temperatures may be attributed to decrease in the mobility of PVA caused by the interactions with continuous glassy gelatin segments.

Unlike gelatin-based composites, addition of sucrose shifted the $T_g$ of pure PVA to the lower temperatures. The presence of single $T_g$ peak in the composites verified the formation of single homogeneous phase in the bulk samples. As a small molecule, sucrose penetrates into PVA network and inhibits the intermolecular interactions, while improving the intramolecular interactions with PVA. Increasing concentration of sucrose disentangles the PVA network more efficiently, thus enhances the mobility of the PVA segments. As the peak position and the intensity of $T_g$ are primarily controlled by the segmental mobility, the observation of the shift in $T_g$ of pure PVA to lower temperatures was indeed as expected. Plasticizing effect of sucrose on PVA was also reported before.[32] Similarly, such segmental interactions can be characterized from the $T_g$ peak in tan $\delta$ curve as seen in Figure 1d.

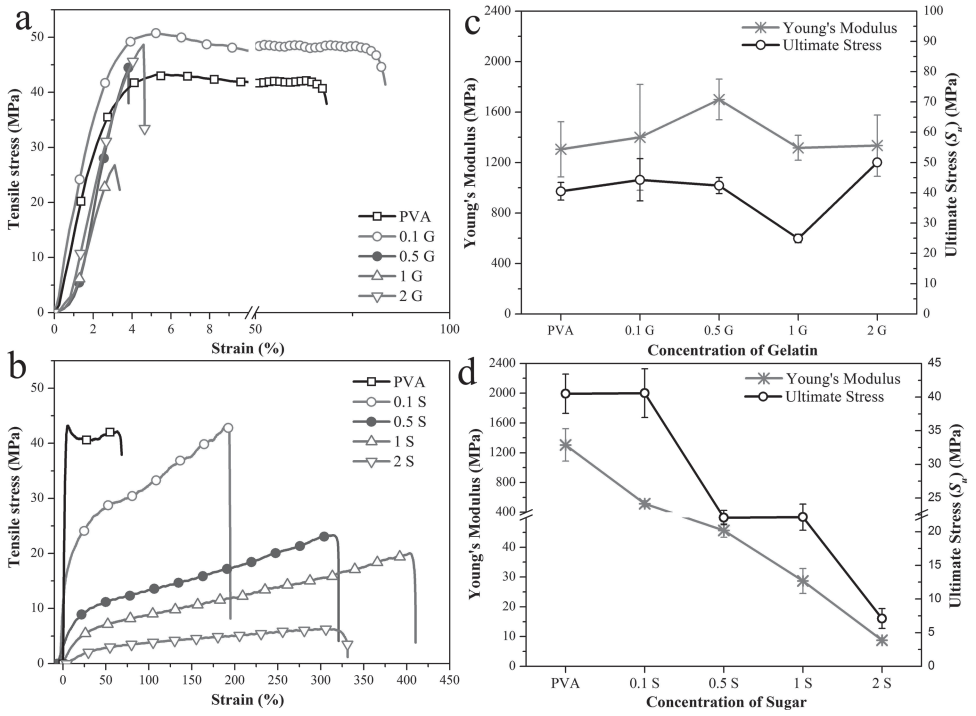


**Figure 2.** a,b) Tensile strength measurements, and c,d) Young's moduli and ultimate stress (MPa) values of PVA/Gelatin composites and PVA/Sugar composites, respectively.

Below room temperature, all PVA/sucrose composites exhibited glassy behavior. In this region, $E'$ did not show any dependence on the temperature. The highest sucrose content showed the highest modulus below room temperature. Similar phenomena was attributed to the reinforcement of the sucrose in PVA matrix below its $T_g$, resulting denser polymer segments and thus, higher glassy modulus.[29] Increasing the concentration of sucrose decreased the extension of the glassy plateau regime and caused substantial decrease in storage modulus in transition regime, in which the crystalline segments of the polymers started to relax and became more flexible. This observation supports the plasticizing effect of sucrose on PVA.

At temperatures above 140 °C, complete reduction in storage modulus of the PVA/sucrose composites was observed. The onset shifted to lower temperatures with increasing sucrose concentration. This phenomena was attributed to the melting of sucrose, which occurs around 186 °C for pure sucrose, and resulted increased mobility. Overall, addition of sucrose to PVA resulted in more elastic composites at temperatures above $T_g$.

Tensile tests were conducted to further characterize the mechanical properties of the polymer composites. The stress-strain curves, Young's modulus and the tensile strain at break of PVA/gelatin composites were compared to pure PVA in **Figure 2**a and b, respectively. The Young's modulus, tensile strength and tensile strain at break measured from the stress-strain curves are listed in **Table 1**.

The stress-strain curve of pure PVA exhibited high tensile strength of 40.5 ± 2.9 MPa followed by yielding and fracture as expected from typical semi-ductile material. According to the stress/strain curves of PVA/Gelatin composites, the strain at break of PVA reduced significantly after addition of gelatin to the composite (Figure 2a). Interactions between PVA and gelatin molecules are expected to be responsible for this behavior, which is discussed in section 3.2. Addition of gelatin in PVA improved the stiffness of pure PVA as expected.[33] The Young's modulus of PVA increased from 1304 MPa to 3022 MPa with gelatin addition of 0.5 wt% (0.1 G). However, the modulus decreased with further increase in the gelatin concentration. The ultimate stress ($S_u$) also followed similar trend with Young's modulus. The tensile strength measurements were performed at room temperature, which is below than $T_g$ of PVA. In this region ($T < T_g$), storage modulus of PVA/gelatin composites observed lower than that of pure PVA (Figure 1). At low concentrations, gelatin may act as reinforcement materials, which results in the increase of the Young's Modulus as observed in 0.1 G sample. However, as the concentration of gelatin become comparable to, or more than,

**Table 1.** Mechanical properties of the samples.

| Sample | Ultimate Stress [MPa] | Tensile Strain at Break [%] | Young's Modulus [MPa] |
|---|---|---|---|
| PVA | 40.5 ± 2.9 | 76 ± 9.2 | 1304.8 ± 218.5 |
| 0.1 G | 115.6 ± 17.1 | 2.6 ± 0.6 | 3022.7 ± 378.7 |
| 0.5 G | 42.4 ± 2.7 | 4.3 ± 0.7 | 1699.9 ± 167.9 |
| 1 G | 41.2 ± 5.3 | 1.9 ± 0.2 | 1384.5 ± 107.8 |
| 2 G | 50.7 ± 12.1 | 3.7 ± 0.9 | 1182.7 ± 64.7 |
| 0.1 S | 40.6 ± 3.6 | 184.4 ± 19.6 | 513.9 ± 40.8 |
| 0.5 S | 22.1 ± 1.1 | 313.7 ± 8.3 | 45.7 ± 2.3 |
| 1 S | 21.7 ± 1.9 | 419.1 ± 22.1 | 28.7 ± 4.2 |
| 2 S | 7.1 ± 1.4 | 333.1 ± 34.5 | 8.7 ± 0.8 |

**Table 2.** Sample notations and chemical composition of the synthesized films.

| Notation | PVA [wt%] | Sucrose [wt%] | Gelatin [wt%] | Ratio |
|---|---|---|---|---|
| PVA | 5 | 0 | 0 | N/A |
| 0.1 G | 5 | 0 | 0.5 | 10:1 |
| 0.5 G | 5 | 0 | 2.5 | 2:1 |
| 1 G | 5 | 0 | 5 | 1:1 |
| 2 G | 5 | 0 | 10 | 1:2 |
| 0.1 S | 5 | 0.5 | 0 | 10:1 |
| 0.5 S | 5 | 2.5 | 0 | 2:1 |
| 1S | 5 | 5 | 0 | 1:1 |
| 2S | 5 | 10 | 0 | 1:2 |

that of PVA, gelatin is likely to form continuous phase; therefore, Young's modulus is expected to decrease back to that of PVA and/or gelatin phases. The strain at fracture decreased significantly with addition of gelatin, which could be attributed to the embrittlement of gelatin. Increase of maximum tensile strength and Young's modulus with increasing concentration of gelatin in PVA is also consistent with previous results.[34]

Addition of sucrose to PVA (0.1 S) resulted in a significant change in the material's behavior from semi-ductile to rubbery (Figure 2c). Lack of yielding behavior in the stress-strain curves of composites represented rubbery nature of the material. The modulus and ultimate stress of PVA reduced from around 1305 MPa and 41 MPa to around 9 MPa and 7 MPa, respectively (**Table 2**). The maximum tensile stress decreased with the additional sucrose, while tensile strain at break increased. The change in mechanical behavior with additions of sucrose is explained in Section 3.2 with chemical interactions between PVA and sucrose.

### 2.2. Chemical Characterization

FTIR was used to characterize the specific chemical interactions between the host PVA matrix and the fillers. In **Figure 3**, the FTIR spectra of the polymer samples are shown. The formation of specific intermolecular interactions through hydrogen-bonding between two or more polymers were responsible for the changes in mechanical properties of the composites. The bands around 2910–2938 $cm^{-1}$ (Figure 3 a and b) correspond to the $–CH_2$ groups streching vibration of PVA. Since these bands were not influenced by addition of the fillers, they remained unchanged for all samples.[35] The broad band between 3200–3300 $cm^{-1}$ in both PVA/gelatin and PVA/sucrose samples was attributed to the –OH groups originated from the intermolecular and/or intramolecular interactions, especially due to the hydrogen-bonding.[36] Increasing intensity of the bands in this region coresponds to the increasing degree of –OH groups.

A shoulder started to appear at 3421 $cm^{-1}$, which is attributed to the streching vibration of –OH groups of PVA bonded to $–NH_2$ groups of gelatin (Figure 3a).[37] This band became more pronounced at higher gelatin concentrations, which indicated the increasing number of interactions between the filler and the matrix. The bands at 3081 $cm^{-1}$ and 2850 $cm^{-1}$ coresponds to the alkyl and aldehyde chains of gelatin, respectively. Both bands became more pronounced at higher concentrations of gelatin as expected. The bands around 1655, 1548 and 1236 $cm^{-1}$ are characteristics of gelatin which are assigned to Amide I (C=O and C–N streching vibration), Amide II (N–H bending vibration) and Amide III (C–N vibration), respectively.[38,39] In the presence of PVA, these bands shifted toward lower wavenumbers of 1634, 1546 and 1228 $cm^{-1}$, respectively. These shifts indicate esterification reactions; thus, confirm good molecular compability between PVA and gelatin.[27,37,38,40] Bands at 1141 and 1085 $cm^{-1}$ correspond to C–C vibrations and C–O streching of secondary alcoholic groups, respectively.[27]

The characteristic absorbance of PVA/sucrose polymer composite is mostly in the lower wavenumbers (Figure 3b). The bands around 1646 and 916 $cm^{-1}$ are attributed to alkene groups. Bending vibrations of C-H groups of sucrose were observed at 1417 $cm^{-1}$ coupled with bending vibrations of O–H at 1327 $cm^{-1}$.

The FTIR analyses implied the fillers are chemically interacting with the PVA network. These chemical interactions

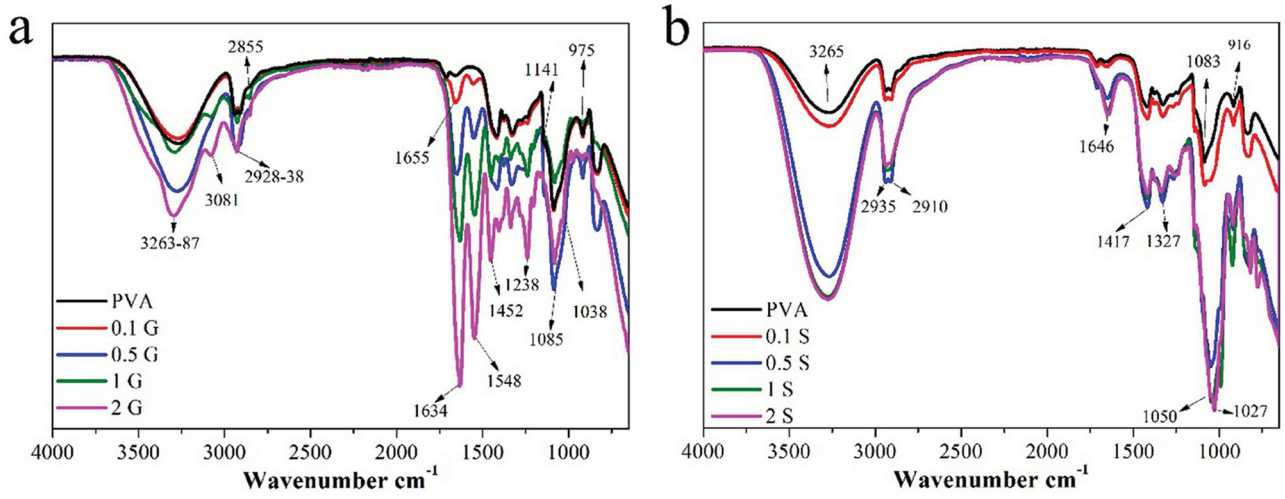


**Figure 3.** FTIR spectra of a) PVA/gelatin samples and b) PVA/sucrose samples 4000–650 $cm^{-1}$.

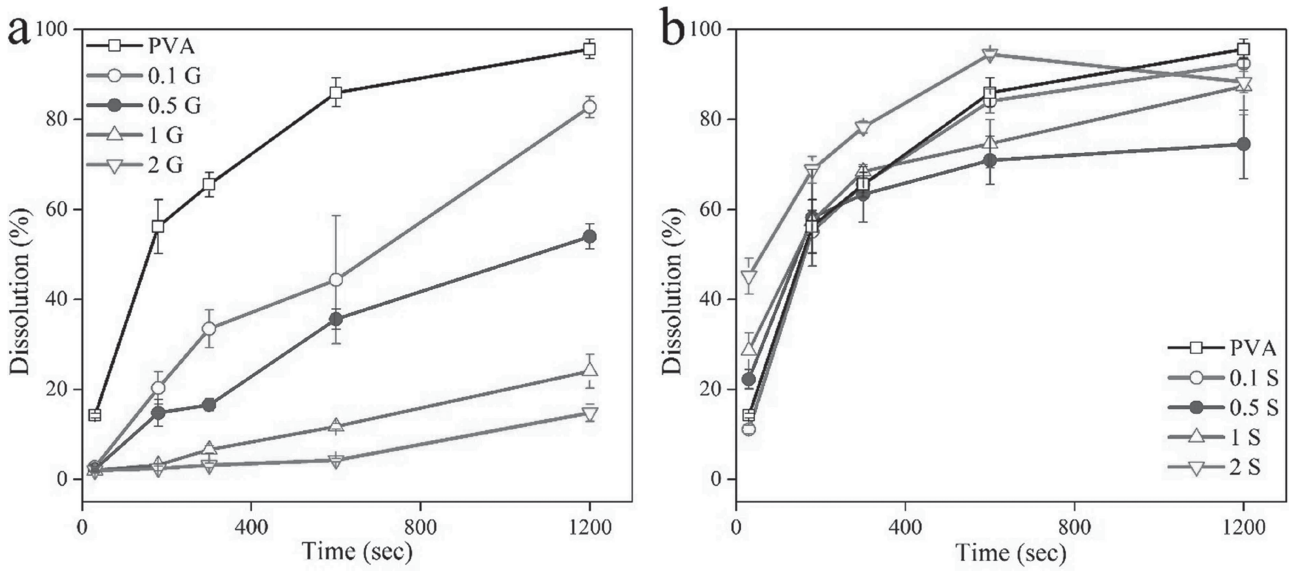


**Figure 4.** Time-dependence dissolution of a) PVA/gelatin and b) PVA/sucrose composites.

determined the superior properties of the polymer composites synthesized in this study. Formation of homogeneous composites by additions of sucrose or gelatin into PVA was confirmed by thermal gravimetric analysis (supplementary data).

### 2.3. Dissolution and Transiency

The polymer composites were completely stable in the ambient conditions for months, without any visible or measurable signs of degradation, or change in properties. As designed, the polymer films underwent a fast degradation followed by dissolution to a significant extent, when exposed to water. Presented in **Figure 4** is the time-dependence dissolution of samples consisting of different ratios of PVA/gelatin and PVA/sucrose.

As shown in Figure 4a, increasing amount of gelatin significantly decreased the solubility of the polymer films. As observed in FTIR analysis, there is a strong interaction between PVA and gelatin (Figure 3a). These interactions, such as hydrogen-bonds and ester bonds, decreased the solubility significantly. Ester bonds, unlike hydroxyl groups of PVA, are not hydrogen-bond donors but acceptors, which by nature decrease water solubility of the material. Thus, water solubility of PVA/gelatin composites decreased as presented Figure 4a.

The PVA/sucrose composites were rapidly dissolved within the first couple of minutes of triggering (Figure 4b). Addition of a small amount of sucrose slightly slowed down the dissolution of the composites, which may be due to the chemical interactions between sucrose and PVA. Nevertheless, increasing the concentration of sucrose to equal or higher concentrations than that of PVA results in a significant decrease in the solubility, suggesting that the interaction between sucrose and PVA increases with the increasing concentration of sucrose. As the composition changes from PVA-dominated to sucrose-dominated in very high concentrations of sucrose, the solubility of composite material increases. Sucrose has significantly higher water solubility than PVA; thus, fast dissolution of the sucrose significantly contributes to the short time dissolution constants

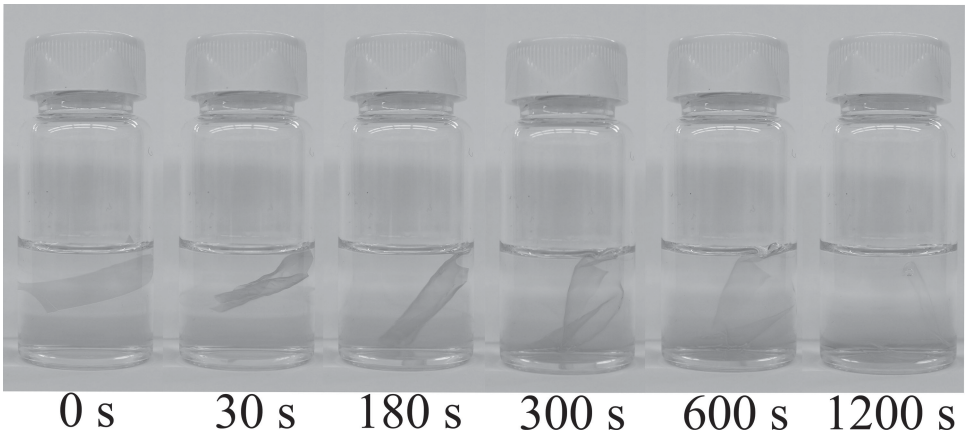


**Figure 5.** Sequential photographs of degradation and transiency of 0.1S film in DI water. 300 s is approximately the time constant for this sample (actual value: 268 s).

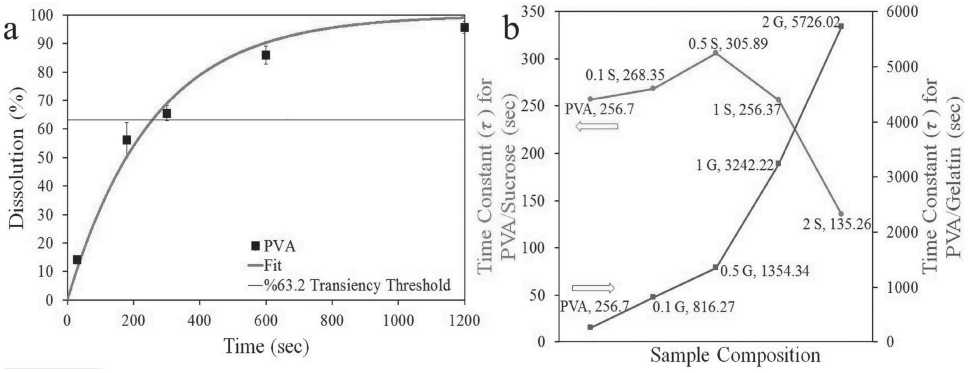


**Figure 6.** Left: Dissolution of PVA as a function of time fitted with an inversed exponential curve at the time constant of 256.7 s. Right: Time constant of samples containing different ratios of sucrose and gelatin. Time constant increases with the increasing ratio of gelatin whereas samples containing equal or more sucrose (relative to PVA) exhibit smaller time constants. Time constant values above 1200 s are not experimentally confirmed and are solely based on theoretical model.

of sucrose-dominated composites. The overall behavior of the composite will be influenced by the crystalline structure of sucrose which lacks physical qualities required for maintaining the mechanical integrity of the film as discussed in Section 3.1.

For films with integrated circuits, degradation and transiency can be defined as points when the integrated electronics cease to function and system is dissolved to an unrecognizable extent, respectively; however, for films without integrated circuits, such as those reported in this work, the terms should be redefined. It was observed that dissolution of the polymer films (except those with high concentrations of gelatin) could be fitted on inversed (cumulative) exponential curves of different time constants; and, the membranes are completely fallen apart and visually unrecognizable as "films" after approximately 60–65% loss of mass. In order to quantify the dissolution and transiency of the polymer films in this work, *transiency* was defined as dissolution of at least 63.2% of the initial mass of the film. Any dissolution less than 63.2% is denoted as *degradation*. The time required to reach the threshold of transiency is denoted as the *time constant*. The data-points for the transiency of the polymer films were fitted with the following equation:

$$T(t) = T_{\max}(1 - e^{-t/\tau}) \quad (1)$$

where $T$ is *dissolution(%)*, $T_{\max}$ is 100 (%), indicating maximum possible dissolution, $t$ is *time* and $\tau$ is the *time constant*. Dissolution of 63.2%, i.e. $T(\tau) = 63.2\%$, is reached when $t = \tau$. Sequential photographs of 0.1S film is presented in **Figure 5**. Photograph at 300 seconds is closest to the time constant for this film (268 seconds). At this stage, the film has lost most of its mass and is mechanically unstable.

Presented in **Figure 6** are dissolution of PVA film as a function of time, fitted with the inversed exponential curve, and the time constants of samples consisting of different PVA-sucrose and PVA-gelatin ratios. Samples consisting of higher concentrations of gelatin (i.e. 0.5G and higher) exhibited linear trends, which were used for calculation of theoretical $\tau$ values reported in Figure 6b. As shown in Figure 6b, increasing concentration of gelatin results in larger time constants, which is due to the chemical interactions between PVA and gelatin as discussed earlier. Contrary to PVA-gelatin samples, addition of sucrose resulted in a rather unpredicted change in time constant, generally lowering it over higher concentrations.

## 3. Conclusion

Polymer composites consisting of different ratios of gelatin or sucrose integrated with PVA matrices were tested for their chemical and physical properties to investigate programmability of such composites for fabrication of transient electronics and platforms for biomedical and military applications. It was demonstrated that dissolution and transiency of the polymer composites could be retarded or enhanced by addition of gelatin or sucrose at different ratios, respectively. It was also observed that PVA/sucrose composites demonstrate superior physical properties, such as higher flexibility, that are desirable for biomedical applications. Interestingly, the dissolution of the polymer composites were fitted with inversed exponential functions of different time constants; with the lower time constants being an indication of faster transiency of the polymer composites. Overall, addition of sucrose showed to decrease the time constant whereas addition of gelatin increased the time constant. It is demonstrated that solubility of the polymer composites can be programmed by manipulation of their composite structures.

## 4. Experimental Section

*Preparation of Polymer Films*: Poly(vinyl alcohol) (PVA) (Mw: 61,000 g mol$^{-1}$, 98.0–98.8 mol% hydrolysis), gelatin and sucrose (Sigma Aldrich) were used as received. To prepare a 5 wt% base PVA solution, 1 g of PVA was added to 20 mL of DI water (R ≥ 18.0 MΩ); 10 µL of 1 M aqueous HCl solution was added to expedite the dissolution. To synthesize films containing various concentrations of sucrose or gelatin, required amount of desired substance (sucrose or gelatin) was added to the base PVA solution and stirred at 120 °C for 1 h, then cooled to room temperature and stirred overnight. Presented in Table 2 is the chemical content of each sample along with the notation used in this study. Solution casting method was used for all composites to fabricate thin polymer films. The casts were dried at ambient conditions for 24 h, then carefully peeled-off from the mold.

*Characterization of Thermal and Mechanical Properties*: All samples were dried at 80 °C for 48 h before the thermal and mechanical

characterization. Thermal stability of the polymer samples was studied using thermo gravimetric analysis (TGA) (TGA Q-50 TA Instruments). The temperature of samples increased from room temperature to 700 °C at a heating rate of 20 °C $min^{-1}$, under nitrogen atmosphere. Samples ($20 \times 8$ $mm^2$) were also characterized for their mechanical properties as a function of temperature, using dynamic mechanical analysis (DMA) (DMA Q-800 TA Instruments) on tensile mode. Temperature sweep tests were carried out between –50 and 250 °C at 1 Hz frequency, with strain amplitude of 0.05% and at a heating rate of 3 °C $min^{-1}$. The storage modulus ($E'$) and damping coefficient ($tan\ \delta$) were measured as a function of temperature. The tensile properties of the polymer films were determined using a tensile testing machine (4502 Instron Universal Testing Machine) at 100 mm $min^{-1}$ crosshead speed. The tests were conducted on rectangular shape thin-film samples with a gauge length of 30 mm. The Young's modulus was calculated using the Bluehill software supplied with the equipment. At least four replicates of each sample were taken, and averaged values are reported as mechanical properties of the composites.

*Infrared Spectroscopy*: Attenuated total reflectance-Fourier transform infrared (ATR-FTIR) spectroscopy (Frontier Perkin Elmer) equipped with single reflection ATR attachment with diamond crystal was used for this study. Samples were placed directly on the ATR crystal. Four scans with a spectral resolution of 4 $cm^{-1}$ were taken at room temperature for each sample. Data was processed by Spectrum 10 software. For each spectrum, an interactive baseline correction with respect to the position of 4000 $cm^{-1}$ was employed.

*Dissolution and Transiency*: Transiency of the polymer films was defined and determined as the ratio of the films' masses before and after exposure to the trigger, deionize (DI) water. The $1 \times 3$ $cm^2$ pieces of polymer films were individually sandwiched in $3 \times 4$ cm aluminum-mesh containers. The mesh containers, containing polymer films, were submersed in DI water for 30, 180, 300, 600, and 1200 s; then dry in ambient for 24 h. The mass of containers and the films were measured and recorded before and after exposing to DI water. All the experiments were repeated three times and results were averaged.

## Supporting Information

Supporting Information is available from the Wiley Online Library or from the author.

## Acknowledgements

This material is based upon work supported in part by the Iowa State University. A portion of this work was supported by a funding from Health Research Initiative and Presidential Initiative for Interdisciplinary Research at Iowa State University. Authors would like to thank Professor Mufit Akinc for his support of this work.

Received: December 16, 2013
Revised: February 9, 2014
Published online: April 1, 2014

[1] M. Berggren, A. Richter-Dahlfors, *Adv. Mater.* **2007**, *19*, 3201.
[2] S. W. Hwang, H. Tao, D. H. Kim, H. Cheng, J. K. Song, E. Rill, M. A. Brenckle, B. Panilaitis, S. M. Won, Y. S. Kim, Y. M. Song, K. J. Yu, A. Ameen, R. Li, Y. Su, M. Yang, D. L. Kaplan, M. R. Zakin, M. J. Slepian, Y. Huang, F. G. Omenetto, J. A. Rogers, *Science* **2012**, *337*, 1640.
[3] a) A. Lendlein, M. Rehahn, M. R. Buchmeiser, R. Haag, *Macromol. Rapid Commun.* **2010**, *31*, 1487; b) J. Frechet, *Prog. Polym. Sci.* **2005**, *30*, 844; c) C. J. Bettinger, Z. Bao, *Adv. Mater.* **2010**, *22*, 651; d) V. K. Rangari, R. Samsur, S. Jeelani, *J. Appl. Polym. Sci.* **2012**, *129*, 1249.
[4] H. Acar, R. Garifullin, L. E. Aygun, A. K. Okyay, M. O. Guler, *J. Mater. Chem. A.* **2013**.
[5] a) Centers for Disease Control and Prevention, *Am. J. Infect. Control.* **1996**, *24*, 380; b) F. B. Mullauer, J. H. Kessler, J. P. Medema, *PLoS ONE.* **2009**, *4*, e1.
[6] a) R. A. Andersen, S. Musallam, B. Pesaran, *Curr. Opin. Neurobiol.* **2004**, *14*, 720; b) C. Mehring, J. Rickert, E. V. S. C. d. Oliveira, A. Aertsen, S. Rotter, *Nat. Neurosci.* **2003**, *6*, 2.
[7] D. H. Kim, J. Viventi, J. J. Amsden, J. Xiao, L. Vigeland, Y.-S. Kim, J. A. Blanco, B. Panilaitis, E. S. Frechette, D. Contreras, *Nat. Mater.* **2010**, *9*, 511.
[8] a) S.-W. Hwang, D.-H. Kim, H. Tao, T.-i. Kim, S. Kim, K. J. Yu, B. Panilaitis, J.-W. Jeong, J.-K. Song, F. G. Omenetto, J. A. Rogers, *Adv. Funct. Mater.* **2013**, *23*, 4087; b) R. Farra, N. F. Sheppard, L. McCabe, R. M. Neer, J. M. Anderson, J. T. Santini, M. J. Cima, R. Langer, *Sci. Transl. Med.* **2012**, *4*, 122ra21.
[9] M. Irimia-Vladu, N. S. Sariciftci, S. Bauer, *J. Mater. Chem.* **2011**, *21*, 1350.
[10] M. Irimia-Vladu, E. D. Głowacki, G. Voss, S. Bauer, N. S. Sariciftci, *Mater. Today* **2012**, *15*, 340.
[11] a) C. Suspene, B. Piro, S. Reisberg, M.-C. Pham, H. Toss, M. Berggren, A. Yassar, G. Horowitz, *J. Mater. Chem. B* **2013**, *1*, 2090; b) J. Kawahara, P. Andersson Ersman, X. Wang, G. Gustafsson, H. Granberg, M. Berggren, *Org. Electron.* **2013**, *14*, 3061; c) K. Svennersten, M. Berggren, A. Richter-Dahlfors, E. W. H. Jager, *Lab on Chip* **2011**, *11*, 3287; d) J. A. Chikar, J. L. Hendricks, S. M. Richardson-Burns, Y. Raphael, B. E. Pfingst, D. C. Martin, *Biomaterials* **2012**, *33*, 1982; e) S. Venkatraman, J. Hendricks, Z. A. King, A. J. Sereno, S. Richardson-Burns, D. Martin, J. M. Carmena, *IEEE Trans. Neural Syst. Rehabil. Eng.* **2011**, *19*, 307; f) X. Strakosas, M. Sessolo, A. Hama, J. Rivnay, E. Stavrinidou, G. G. Malliaras, R. M. Owens, *J. Mater. Chem. B* **2014**; g) Z.-Q. Feng, J. Wu, W. Cho, M. K. Leach, E. W. Franz, Y. I. Naim, Z.-Z. Gu, J. M. Corey, D. C. Martin, *Polymer* **2013**, *54*, 702; h) F. Patolsky, B. P. Timko, G. Yu, Y. Fang, A. B. Greytak, G. Zheng, C. M. Lieber, *Science* **2006**, *313*, 1100; i) P. Andersson Ersman, D. Nilsson, J. Kawahara, G. Gustafsson, M. Berggren, *Org. Electron.* **2013**, *14*, 1276.
[12] M. Sessolo, D. Khodagholy, J. Rivnay, F. Maddalena, M. Gleyzes, E. Steidl, B. Buisson, G. G. Malliaras, *Adv. Mater.* **2013**, *25*, 2135.
[13] X. Cui, V. A. Lee, Y. Raphael, J. A. Wiler, J. F. Hetke, D. J. Anderson, D. C. Martin, *J. Biomed. Mater. Res.* **2001**, *56*, 261.
[14] C. J. Bettinger, Z. Bao, *Adv. Mater.* **2009**, *22*, 651.
[15] H. Acar, R. Genc, M. Urel, T. S. Erkal, A. Dana, M. O. Guler, *Langmuir* **2012**, *28*, 16347.
[16] M. Irimia-Vladu, P. A. Troshin, M. Reisinger, L. Shmygleva, Y. Kanbur, G. Schwabegger, M. Bodea, R. Schwödiauer, A. Mumyatov, J. W. Fergus, *Adv. Funct. Mater.* **2010**, *20*, 4069.
[17] a) H. Wang, Z. M. Shi, K. Yang, *Adv. Mater. Res.* **2008**, *32*, 207; b) J. Reifenrath, D. Bormann, A. Meyer-Lindenberg, *Magnesium Alloys as Promising Degradable Implant Materials in Orthopaedic Research*, InTech, Ukraine **2011**, 93; c) S. Shrestha, *Surf. Eng.* **2010**, *26*, 313.
[18] a) C. Zhong, Y. Deng, A. F. Roudsari, A. Kapetanovic, M. Anantram, M. Rolandi, *Nat. Commun.* **2011**, *2*, 476; b) Y. Deng, E. Josberger, J. Jin, A. F. Rousdari, B. A. Helms, C. Zhong, M. Anantram, M. Rolandi, *Sci. Rep.* **2013**, *3*.
[19] a) M. Irimia-Vladu, E. D. Głowacki, P. A. Troshin, G. Schwabegger, L. Leonat, D. K. Susarova, O. Krystal, M. Ullah, Y. Kanbur, M. A. Bodea, V. F. Razumov, H. Sitter, S. Bauer, N. S. Sariciftci, *Adv. Mater.* **2012**, *24*, 375; b) E. D. Glowacki, M. Irimia-Vladu, S. Bauer, N. S. Sariciftci, *J. Mater. Chem. B* **2013**, *1*, 3742.
[20] A. B. Mostert, G. R. Hanson, T. Sarna, I. R. Gentle, B. J. Powell, P. Meredith, *J. Mater. Chem. B* **2013**, *117*, 4965.
[21] C. Legnani, C. Vilani, V. Calil, H. Barud, W. Quirino, C. Achete, S. Ribeiro, M. Cremona, *Thin Solid Films.* **2008**, *517*, 1016.

[22] X. Wang, J. A. Kluge, G. G. Leisk, D. L. Kaplan, *Biomaterials* **2008**, *29*, 1054.
[23] X. Hu, K. Shmelev, L. Sun, E.-S. Gil, S.-H. Park, P. Cebe, D. L. Kaplan, *Biomacromolecules* **2011**, *12*, 1686.
[24] a) R. Montazami, C. M. Spillmann, J. Naciri, B. R. Ratna, *Sens. Actuat. A* **2012**, *178*, 175; b) R. Montazami, S. Liu, Y. Liu, D. Wang, Q. Zhang, J. R. Heflin, *J. Appl. Phys.* **2011**, *109*, 104301; c) R. Montazami, V. Jain, J. R. Heflin, *Electrochim. Acta* **2010**, *56*, 990; d) S. Liu, R. Montazami, Y. Liu, V. Jain, M. Lin, X. Zhou, J. R. Heflin, Q. M. Zhang, *Sens. Actuat. A* **2010**, *157*, 267; e) S. Liu, R. Montazami, Y. Liu, V. Jain, M. Lin, J. R. Heflin, Q. M. Zhang, *Appl. Phys. Lett.* **2009**, *95*, 023505.
[25] a) E. Chiellini, P. Cinelli, E. G. Fernandes, E.-R. S. Kenawy, A. Lazzeri, *Biomacromolecules* **2001**, *2*, 806; b) E. Bradbury, C. Martin, *Proc. Roy. Soc. London A* **1952**, *214*, 183.
[26] A. Bigi, S. Panzavolta, K. Rubini, *Biomaterials* **2004**, *25*, 5675.
[27] S. M. Pawde, K. Deshmukh, *J. Appl. Polym. Sci.* **2008**, *109*, 3431.
[28] a) G. Cherian, A. Gennadios, C. L. Weller, P. Chinachoti, **1995**; b) M. T. Kalichevsky, E. M. Jaroszkiewicz, J. M. V. Blanshard, *Polymer* **1993**, *34*, 346.
[29] M. T. Kalichevsky, E. M. Jaroszkiewicz, J. M. V. Blanshard, *Int. J. Biol. Macromol.* **1992**, *14*, 257.
[30] J.-S. Park, J.-W. Park, E. Ruckenstein, *J. Appl. Polym. Sci.* **2001**, *82*, 1816.
[31] M. G. Cascone, *Polymer Int.* **1997**, *43*, 55.
[32] a) R. P. Westhoff, W. F. Kwolek, F. H. Otey, *Starch – Stärke* **1979**, *31*, 163; b) I. Arvanitoyannis, I. Kolokuris, A. Nakayama, N. Yamamoto, S.-i. Aiba, *Carbohydr. Polym.* **1997**, *34*, 9.
[33] V. Merkle, L. Zeng, W. Teng, M. Slepian, X. Wu, *Polymer* **2013**, *54*, 6003.
[34] E.-E. Hago, X. Li, *Adv. Mater. Sci. Eng.* **2013**, *2013*, 8.
[35] T. M. R. Miranda, A. R. Gonçalves, M. T. P. Amorim, *Polymer Int.* **2001**, *50*, 1068.
[36] G. Andrade, E. Barbosa-Stancioli, A. P. Mansur, W. L. Vasconcelos, H. Mansur, *J. Mater. Sci.* **2008**, *43*, 450.
[37] Z. Dong, Q. Wang, Y. Du, *J. Membr. Sci.* **2006**, *280*, 37.
[38] C. Xiao, H. Liu, Y. Lu, L. Zhang, *J. Macromol. Sci., Part A: Pure Appl. Chem.* **2001**, *38*, 317.
[39] H. Acar, R. Garifullin, M. O. Guler, *Langmuir.* **2011**, *27*, 1079.
[40] Y. Jia-hui, D. Yu-min, Z. Hua, *Wuhan Univ. J. Nat. Sci.* **1999**, *4*, 476.